

USING 2D DENTAL GEOMETRIC MORPHOMETRICS TO
IDENTIFY MODERN *PEROGNATHUS* AND *CHAETODIPUS*
SPECIMENS (RODENTIA, HETEROMYIDAE)

by

MEGAN RENEE WYATT

A THESIS

Presented to the Department of Biology,
the Department of Earth Sciences,
and the Robert D. Clark Honors College
in partial fulfillment of the requirements for the degree of
Bachelor of Science

May 2020

An Abstract of the Thesis of

Megan Wyatt for the degree of Bachelor of Science
in the Department of Biology and the Department of Earth Sciences
to be taken May 2020

Title: Using 2D Dental Geometric Morphometrics to Identify Modern *Chaetodipus*
and *Perognathus* Specimens (Rodentia, Heteromyidae)

Approved: Samantha Hopkins, Ph.D.
Primary Thesis Advisor

The Heteromyidae (pocket mice and kangaroo rats) are a group of extant small rodents abundant in North American Cenozoic fossil assemblages. Two genera of heteromyids, *Chaetodipus* and *Perognathus*, share similar tooth morphology whose fossils are distinguished using skull shape and body size estimates. Previous genetic studies show these extant genera likely diverged in the early Miocene (~20 million years ago). However, the *Chaetodipus* fossil record starts in the Pleistocene (~2 million years ago) while the *Perognathus* fossil record begins in the middle Miocene, near the time suggested by molecular divergence. Other studies found these two genera are not distinguishable from each other using descriptive dental morphology alone. In this study, I asked whether two-dimensional geometric morphometrics on complete dentition and isolated premolars can accurately identify *Chaetodipus* and *Perognathus* specimens at the genus and species-level. I developed a landmarking scheme based on features that are consistent through wear, are recognizable in the fossil record, and could be subset for analyses on individual molars. I landmarked the occlusal surface of the upper and lower tooth rows of modern *Chaetodipus* (n=83) and *Perognathus*

specimens (n=80), including 12 of the 26 extant species across the two genera. We used the R packages “geomorph” and “Morpho” to run a canonical variates analysis to investigate whether principal component variation could predict known taxonomic identifications. The morphospace using complete dentition can identify specimens to genus with 90-92% accuracy and to species with more variable accuracy. Similarities in body size and biogeographic ranges explained genus-level misidentification while phylogenetic relationships explained species-level misidentification. Specifically, *Perognathus parvus*, the largest *Perognathus* species in the analysis, was most frequently misidentified as *Chaetodipus*. I found an isolated premolar provides sufficient information for genus-level identification (69%-84% accuracy), but not for species-level identification (26%-56% accuracy). The morphospace suggests the anterior-posterior length and transverse width ratios of the premolars are diagnostic for genus identification. This morphospace of modern specimens can be used to identify the fossil dentition of *Chaetodipus* and *Perognathus* specimens already in museum collections and refine our existing knowledge of heteromyid evolutionary history.

Acknowledgments

I would like to thank Samantha Hopkins for introducing me to vertebrate paleontology and guiding me through this project. I would also like to thank Edward Davis, Dana Reuter, and Paul Z. Barrett for help with data analysis and data visualization. Thank you to Kellum Tate-Jones for guidance and support while collecting data at the University of California Museum of Paleontology and the Museum of Vertebrate Zoology. Thank you to Chris Conroy at the Museum of Vertebrate Zoology and Patricia Holroyd at the University of California Museum of Paleontology for specimen access. I would also like to thank Jonathan Calede, Tara Smiley, P. David Polly, and Natasha Vitek for helpful discussions and input on the project. Thank you to the University of Oregon Clark Honors College, the University of Oregon Department of Earth Sciences, the Museum of Natural and Cultural History, the Paleontological Society, and the Geological Society of America for funding data collection and conference travels. Thank you to the entire University of Oregon Vertebrate Paleontology Lab for input and support on this project. Lastly, thank you to my parents for their support of my undergraduate education.

Table of Contents

Introduction	1
Methods	7
Data Collection	7
Data Analysis	10
Results	13
Discussion	17
Figures and Tables	21
Bibliography	36

List of Figures and Tables

Figure 1. Estimated divergence of <i>Chaetodipus</i> and <i>Perognathus</i> compared to the fossil record (from Hafner et al., 2007)	21
Figure 2: Boxplot of specimen lower tooth row length	22
Figure 3. Tooth cusp terminology for molars and premolars	23
Table 1: List of specimens used in the analysis	24
Figure 4: Landmarking scheme for upper molars and lower molars	25
Table 2: Description of landmarks in Figure 4	26
Figure 5: Generalized Procrustes of the upper tooth row	27
Figure 6: Generalized Procrustes of the lower tooth row	27
Figure 7: PCA of the upper molars	28
Figure 8: PCA of lower molars	29
Table 3: Summary table of canonical variates analyses	30
Table 4. Summary of misidentification from genus-level cross-validation	31
Table 5: Summary table of species-level classification accuracy from complete dentition without size	32
Table 6: Summary table of species-level classification accuracy from complete dentition with size	33
Figure 10: Canonical variates analysis of species complete dentition with size	35

Introduction

The fossil record is key to understanding the evolutionary relationships of modern animals. Molecular phylogenetic trees provide information about the relationships of extant taxa, but without information from the fossil record, we cannot accurately estimate divergence times or understand morphological trait evolution in those taxa (Slater et al., 2012; Rabosky, 2009; Losos, 2011). Both paleontologists and evolutionary biologists rely on accurate fossil identifications to study the evolutionary history of a lineage. Paleontologists can identify taxa from fossils on the assumption that there is a phylogenetic signal in morphological features. Sometimes, the features that show identifiable morphological differences between taxa are not the features that preserve in the fossil record. In these cases, a disagreement arises between the known fossil record and estimated occurrences from molecular phylogenetics.

This study focuses on the extant genera of pocket mice *Chaetodipus* and *Perognathus*. Pocket mice and kangaroo rats (the family Heteromyidae) are abundant in North American Cenozoic fossil assemblages. Their fossil remains are mostly isolated teeth and occasional jaws. There is still a debate on the relationship between *Chaetodipus* and *Perognathus*. One molecular phylogenetic study shows that the genera are sister taxa (Hafner et al., 2007), while another study suggests *Chaetodipus* and *Perognathus* are most distantly related, with *Perognathus* being the stem group to *Chaetodipus* (Fabre et al., 2012). Both studies agree that the two genera diverged in the early Miocene based on tip-dated phylogenetic trees (Fig. 1). The first known fossil occurrence of *Perognathus* is in the middle Miocene (Reynolds, 1992), close to the expected divergence of these two genera. However, the earliest known fossil occurrence

of *Chaetodipus* is in the Pleistocene (Ayer, 1936), nearly 20 million years after the calculated appearance from molecular phylogenies. There is a clear gap between where we expect to find fossil *Chaetodipus* specimens based on estimated divergence times and where we have identified fossil *Chaetodipus* specimens in museum collections. The current fossil record and this divergence estimate cannot both be true. Either the first *Chaetodipus* fossil is genuinely in the Pleistocene, and the molecular estimate requires fossil data to be accurately calibrated; or the first *Chaetodipus* specimen does appear in the Miocene and we need to develop an accurate way to identify Miocene heteromyid specimens already in museum drawers. To determine which hypothesis is correct, we need to be able to accurately identify fossil *Chaetodipus* specimens based on dentition.

The known fossil *Chaetodipus* specimens from the Pleistocene and Holocene are identified using two methods: comparative morphology of the crania and body size. The interparietal and auditory bullae on the posterior end of the cranium were the first skeletal features used to morphologically distinguish *Chaetodipus* and *Perognathus* as sub-genera in 1889 before genetic data were available (Merriam, 1889). This finding was from complete, modern specimens in natural history collections. While the interparietal provides a clear feature to identify genera, it is rare to find a heteromyid skull in the fossil record. Heteromyid skulls are fragile and require extraordinary conditions to preserve in the fossil record. However, one of these rare heteromyid skulls is the earliest known *Chaetodipus* fossil from Pleistocene Williams Cave in Texas, identified based on “the shape and size of the interparietal” (Ayer, 1936, p. 607). Additional studies of fossil heteromyid skulls have also used the interparietal as a diagnostic feature (Korth, 2008). However, relying only on cranial morphology to

distinguish *Chaetodipus* and *Perognathus* does not allow us to identify most of their fossil record.

The more common method of distinguishing *Chaetodipus* from *Perognathus* in Pleistocene and Holocene faunas is by body size. The extant *Chaetodipus* species are, on average, larger than the extant *Perognathus* species (Fig. 2). The exception is *Perognathus parvus*, whose average body size lies in the middle of the overall average for all *Chaetodipus* species. On the order of millions of years, size is more plastic and changes independently of phylogenetic relationships. Therefore, using specimen size is not an effective way to identify *Chaetodipus* and *Perognathus* specimens over 20 million years.

The abundant preservation of isolated teeth in the rodent fossil record leaves cheek tooth size and shape as the primary basis for fossil rodent identification (Wood, 1935). Common identifiable characters include crown height, tooth size, and the morphology of occlusal lophs and cusps (Barnosky, 1986; Korth, 1987; Wood, 1933). Both *Chaetodipus* and *Perognathus* specimens have similar low crown heights and the same bilophodont dentition with three cusps on each loph (Fig. 3). Because of these similarities in macro-morphology, previous studies have thought to use linear morphometrics to identify heteromyid genera. Linear morphometrics utilizes several measurements of the teeth as independent characters for identification. For example, a study done by Carrasco (2000) used 16 dental measurements of *Dipodomys* specimens to investigate whether linear measurements could reliably identify the teeth of modern *Dipodomys* species, another heteromyid genus. Carrasco (2000) found that linear measurements alone produced many significant false-positive identifications and are not

reliable for identifying *Dipodomys* species. This poor identification is because linear measurements are strongly correlated to body size, which varies independently of phylogenetic relationships. What linear morphometrics do not capture is the overall shape and covarying ratios of the teeth, a gap of knowledge that geometric morphometrics fills.

Geometric morphometrics is the quantitative study of shape variation within taxa. Landmark-based morphometrics allows one to analyze morphological variation on a two-dimensional image or a three-dimensional scan (Zelditch, 2004). This technique has been effective in distinguishing morphologically similar mammalian taxa in the past. McGuire (2011) showed that two-dimensional geometric morphometrics could distinguish five extant genera of voles that were previously thought to be indistinguishable from each other. She used several different morphometric approaches, including standard landmarks and a combination of landmarks and semi-landmarks, and with and without size included. She found that the semi-landmark curves were too variable to be taxonomically useful and that only using landmarks with specimen size provided accurate taxonomic identification. Calede and Glusman (2017) used two-dimensional geometric morphometrics to identify modern and fossil Geomyidae (pocket gophers) specimens. In their analysis, they used a combination of landmarks and semi-landmarks to capture the shape of the occlusal surface of the molars. As a hypsodont taxon, the geomyid teeth wear into enamel lakes and are identified based on the shape of the occlusal surface of isolated molars. The study used a canonical variates analysis on the principal components from a Procrustes fit of the taxa of interest. The study found 86.7 to 100% classification accuracy using isolated premolars. The study also

confirmed previous qualitative analyses of tooth shape and found specimens requiring taxonomic revisions. These studies show that using landmark-based geometric morphometrics has been successful at identifying modern and fossil rodent taxa. No one has yet explored landmark-based morphological analyses of heteromyid dentition to identify modern and fossil specimens.

The focus of the study is whether two-dimensional geometric morphometrics on complete dentition or an isolated premolar accurately identify *Chaetodipus* and *Perognathus* specimens at the genus and species levels. I expected landmarks on complete dentition would provide enough information for genus-level identification and be able to identify some, but not all species. Phylogenetic signal in morphology allows paleontologists to identify fossils. For heteromyid rodents, it is common to use morphology to identify specimens to genus and size to identify specimens to species (Wood, 1935). I expect species with distant common ancestors will be better identifiable in the morphospace. If there is phylogenetic signal in the morphology, then sister taxa should be more morphologically similar to each other. I also expect species with overlapping biogeographic ranges will have a higher classification accuracy. Species that co-occur in the same locality cannot occupy the same ecological niche. This ecological principal means species that do not overlap in their biogeographic range have the opportunity to occupy similar niches and, therefore, could express similar dental morphology. I also expect the morphospace from just the premolar will provide enough information for genus-level identification, but not species-level identification, based on the limited morphological variation one tooth can provide. I expect size will improve both the genus and species-level classification accuracy because the modern

specimens can be identified using size at the genus-level. Size is also a common reasoning for identifying new rodent species (Wood, 1935). I expected phylogenetic relationships to be the best predictors of misidentification. If this is correct, it will suggest morphology reflects phylogenetic relationships of specimens more than biogeography or body size.

Methods

Data Collection

I used a DinoLite Edge Digital Microscope (Dunwell Tech, Inc.) to take photos of the occlusal surface of the upper and lower molars of extant *Perognathus* and *Chaetodipus* specimens from the Museum of Vertebrate Zoology (MVZ) (Table 1). I included six of the nine extant species of *Perognathus* and six of the 17 extant *Chaetodipus* species in this study. To avoid dramatic differences between specimens based on tooth wear, I only took photos of specimens with complete dentition and young adult wear. Young adult wear is characterized by having distinguishable medial cusps on the premolar, distinguishable metaloph and protoloph on the first and second molar, and a distinguishable loph shape on the third molar (Hoffmeister and Lee, 1967). For ease of landmarking, I focused arbitrarily on the lower left and upper right tooth rows to photograph. Modern *Perognathus* and *Chaetodipus* are both brachydont (low-crowned) taxa, so the crown height would not be a diagnostic character for identification. I did not photograph the lingual and labial sides of the molars as it would be necessary to study crown height because it would not aide genus-level identification. I chose the species with at least ten young adult specimens in the museum to photograph to provide an adequate sample size for analyzing species identification. However, one species, *Perognathus flavescens*, was represented in the end by only nine individuals.

After collecting photos, I compiled a TPS file using tpsUtil v. 3.1.3, and I landmarked the images using tpsDig v. 2.31 (Rohlf, 2010). The images were magnified

20-25 times the original specimen size for landmark placement. I developed a landmarking scheme based on features that identify heteromyid fossils, are consistent through wear, recognizable in the fossil record, and could be subset for further analysis of individual molars. Through wear, the upper molar loph unite lingually, forming a “U” shape, and the lower molar loph unite medially, forming an “H” shape. The anterior loph of the premolar has a reduced number of cusps, one on the upper and two on the lower premolar. The lower premolar loph unite medially, forming a characteristic “X” shape in the enamel. The most worn fossil heteromyid teeth form “enamel lakes,” meaning the only feature that remains is an outline of enamel on the outer edge of the tooth with exposed dentin inside (Lindsey, 1972). Because worn teeth with exposed dentin are common in the fossil record, I did not landmark any cusps, but instead focused on the loph, placing landmarks only on the edges of the teeth.

The landmarking scheme captured the labial and lingual enamel edge of the loph to represent the transverse widths of the teeth. In the lower molars, I chose to capture the asymmetrical shape of the lower molars by landmarking but also the enamel edge of the protostylid-protoconid junction (Fig 4b). In the upper molars, I also captured the buccal union of the metaloph and protoloph, usually seen as the tip of a “V” shape in very worn molars. On the upper premolar, I chose to landmark the protoloph on the edge of the tooth instead of the occlusal surface (Fig 4a). The upper premolar protoloph is conical, meaning it is wider at the root than on the occlusal surface. Less worn upper premolars have pointed protoloph while very worn teeth have protolophs composed of large circles of enamel. By landmarking the edge of the tooth instead of the occlusal surface, the wear stage of a specimen will not change the

landmarked proportion of the premolar protoloph. On the lower premolar, I wanted to capture the “X” shape that is diagnostic of heteromyid dentition. To do this, I placed eight landmarks, four on the outer corners, and four to capture the medial union of the lophs. I chose not to use semi-landmarks (landmark curvature) because I suspected the curvature of the molars might change with wear stages in heteromyid rodents. There are 20 total landmarks on the upper tooth row and 22 on the lower tooth row (Fig. 4 and Table 2).

The first and last teeth in the tooth row are the most variable in mammal taxa (Gingerich, 1974). Specifically, the fourth premolar is the most diagnostic tooth for identifying fossil heteromyid specimens because it is more variable than the other molars (Wood, 1935). The rodent fossil record contains many isolated teeth, and standard screen-washing techniques used to collect these teeth often do not capture the third molar, which is smaller in diameter than the standard mesh size. Therefore, I chose to run analyses using only the premolar landmarks, simulating having only a premolar available in the fossil record.

I ran additional analyses to investigate non-biological sources of error in the final classification accuracies. One, I tested the error in the consistency of my landmark placement. To do this, I repeated the landmarks on 3 *Perognathus* and 3 *Chaetodipus* specimens five times and ran a Procrustes ANOVA to test the similarity between repeated specimens as a measure of landmarking error. The Procrustes ANOVA on the repeated specimens showed a 7.08% landmarking error for the upper tooth row and an 8.54% landmarking error for the lower tooth row, which is negligible compared to the classification accuracies. I also tested if differences in sample size influenced species-

level accuracy. Because museum collections held hundreds of specimens of some species and few specimens of other species, I was able to collect more specimen images of some species and not others. I used a linear regression to test if the species classification accuracy is correlated with sample size. These tests found no correlation between species sample size and species-level classification accuracy. Another possibility is that the difference in the number of landmarks between the upper and lower tooth row is influencing the classification accuracies. To test whether additional landmarks affected the classification accuracy, I removed landmarks 4 and 8 (two medial landmarks) from the lower premolar and ran the general Procrustes analysis, PCA, and CVA without size on the lower tooth row to investigate if the overall genus-level classification accuracy changed. When removing two landmarks from the lower premolar, the lower tooth row classification accuracy only drops 1%. This minor decrease in accuracy means the additional landmarks on the lower molars are not contributing substantially to the increased classification accuracy of the lower molars.

Data Analysis

Using the “gpagen” function from the “geomorph” R package (Adams and Otárola-Castillo, 2013), I ran Generalized Procrustes analyses separately on the upper and lower toothrows to normalize the landmark coordinates around a centroid size and shape to account for differences in orientation and scaling of the photographs. The final normalized Procrustes scores from these analyses demonstrate which landmarks were contributing the most biological variability. Using the “plotTangentSpace” function from the same R package, I used the Procrustes coordinates to run two separate

principal components analyses (PCA) on the upper and lower teeth. The PCA reduces the dimensions and summarizes the morphological variation in the dataset into a morphospace to inform identifiable characters. The PCA calls the axis that accounts for the most morphological variation principal component 1 and adds perpendicular axes until all the variation is accounted for. Using the “CVA” function in the R package “Morpho” (Schlager, 2017), I used the principal component axes that accounted for at least 3% of the variation to run a Canonical Variates Analysis (CVA). The CVA uses the PCA morphospace to produce a model for predicting group membership from continuous variables. I included a jackknife cross-validation test in the CVA, which removes one specimen and identifies it based on the model. The number of correctly identified specimens provides the final classification accuracy. I ran multiple CVAs using different amounts of morphological information in order to determine how much information was necessary for taxonomic information. I used datasets starting with the complete dentition (an upper and lower tooth row), then upper or lower tooth row alone, and finally isolated upper or lower premolars. For each of these datasets, I tested both the genus-level classification between *Perognathus* and *Chaetodipus* and species-level classification of the 12 species included in this study.

While the Generalized Procrustes analysis produces a centroid size for each specimen, specimen size is not a variable in the PCA or CVA in standard geometric morphometric analyses (Webster and Sheets, 2010). Because size has so commonly been used to distinguish *Chaetodipus* and *Perognathus* in modern samples, I reran each canonical variates analysis with size included, to test whether size was critical to genus

or species identification. To add size to the analysis, I used a new R function from Smith and Wilson (2017) that incorporates centroid size into the PCA and CVA.

Previous studies using geometric morphometrics have discovered that the first principal component axis is frequently correlated to size because of the influence of allometry is pervasive in biological systems (Klingenberg, 2016). I ran a linear regression of the specimen centroid size from the Procrustes analysis versus principal component 1 to visualize any allometric correlation between the first principal component and specimen size.

Results

The visualized Generalized Procrustes fit around the centroid confirms the fourth premolar and third molar are the most variable group of landmarks in both the upper and lower tooth rows (Fig. 5 and Fig. 6). This confirms the previous observations that the first and last teeth in the tooth row (the fourth premolar and third molar) are the most variable and potentially diagnostic in heteromyid rodents (Wood, 1935).

The PCA of the upper tooth row reveals the relative size and rotation of the premolar and the third molar is the first principal component of 36 principal component axes (Fig. 7). The PCA of the lower tooth row reveals the relative length of the lophs on the first molar and second molar account for 18% of the variation. In comparison, the relative height of the lophs on the lower premolar accounts for 12% of the total variation with 40 total principal components (Fig. 8). There is no correlation between the first principal component axis scores and specimen centroid size in the analyses without size included. This means that no allometric characters are indirectly influencing the morphological variation represented in the first principal component.

The CVA identified the complete (upper and lower) dentition correctly to genus 91% of the time without size, and 92% with size (Table 3). When looking at the classification of each specimen, *Perognathus parvus* specimens were the most often misidentified as *Chaetodipus* specimens (Table 4). 4 out of 16 *Perognathus parvus* specimens were misidentified without size, and 3 out of 16 were misidentified with size. The only other species that had three or more misidentifications in the genus-level analysis were *Chaetodipus baileyi* and *Chaetodipus hispidus* in the analysis without size.

For identifying the species using complete dentition, every *Perognathus flavescens* specimen was correctly identified with and without size (Table 5 and 6). However, the worst classification accuracy to species is *Perognathus inornatus* with only 4 out of 14 correctly identified without size; yet, this was resolved with size with 8 out of 14 specimens correctly identified (Table 5 and 6). Another species, *Chaetodipus californicus*, also did poorly with only 4 out of 11 correctly identified without size and 6 out of 11 correctly identified with size (Tables 5 and 6).

Using only the upper tooth row, the cross-validation accuracy to genus was 87% with size and 82% without size (Table 3). *Perognathus parvus*, the largest *Perognathus* species, and *Perognathus inornatus*, a medium-sized *Perognathus* with a similar body size to the small *Chaetodipus* species, had the highest misidentification rate with 6 or 7 incorrect identifications with and without size (Table 4). There were no other species with more than two misidentifications in the genus-level analysis with size. *Chaetodipus baileyi* and *Chaetodipus hispidus*, two of the large *Chaetodipus* species, had four misidentified specimens in the genus-level analysis without size.

When identifying species using only the upper tooth row, the best species was *Chaetodipus intermedius* with 11 out of 13 specimens correctly identified to species. *Perognathus inornatus* was the worst group with only 5 out of 14 specimens correctly identified both with and without size (Tables 5 and 6).

Using only the lower tooth row, the cross-validation accuracy to genus was 87% with size and 86% without size (Table 3). *Perognathus inornatus* had the highest misidentification rate with seven misidentifications at the genus-level, both with and without size (Table 4). *Chaetodipus penicillatus* also had trouble with five

misidentifications with and without size, and *Perognathus parvus* had three misidentifications with and without size. *Perognathus inornatus* and *Chaetodipus penicillatus* fall in the same size category (Fig. 2).

For the species-level analysis using only the lower tooth row, *Perognathus flavescens* had the highest classification accuracy with 8 out of 10 species correctly identified to species without size and 9 with size (Tables 5 and 6). *Perognathus parvus* did the worst with only 3 out of 10 correctly identified to species with and without size.

Using just an isolated upper premolar yielded 84% genus identification accuracy with size and 79% accuracy without size (Table 3). The lower premolar yielded 79% genus identification accuracy with size and 69% accuracy without size. With only about a 10% to 15% drop in classification accuracy, these analyses on the isolated premolars show that not only is the premolar providing most of the information included in the entire tooth row, but it has enough variation for genus-level identification.

For identifying species, the upper premolar had an overall classification accuracy of 56% with size (not using the cross-validation) and 27% without size (using the cross-validation). The lower premolar had an overall classification accuracy of 38% with size and 26% without size. For both of the premolars, none of the individual species-level analysis had higher than 67% classification accuracy for a single species. This shows that while the premolars provide enough information for genus-level identification, they do not provide enough information for species-level identification,

Including size in the analysis had a more important impact on the species-level analyses than the genus-level analyses. There was only one case where a species from one genus was commonly mistaken for a species in a different genus, *Chaetodipus*

penicillatus and *Perognathus inornatus*, which have very similar body size ranges. All of the cases where three or more specimens of a species were assigned to the same incorrect species were corrected with the inclusion of size. The body size range of a species was the most common explanation for misidentification when comparing the size, phylogenetic relationships, and biogeographic ranges of each species. The x-axis of the species-level CVA shows that the *Perognathus* species have mostly negative values and *Chaetodipus* species have mostly positive value indicating that CV1 (the primary axis of differentiation) is distinguishing the genera (Fig. 9 and 10). When including size, *Perognathus parvus* become more positive, closer to the *Chaetodipus* specimens (Fig. 10). *Perognathus parvus* is the only specimen with a body size range between the smallest and largest *Chaetodipus* species. In this case, size is adding noise to the species-level classification accuracy.

Discussion

It is evident from the analyses that two-dimensional geometric morphometrics on complete dentition can accurately identify *Chaetodipus* and *Perognathus* specimens at the genus level and species level. Two-dimensional geometric morphometrics on an isolated premolar, however, can accurately identify specimens to genus, not species. Body size and biogeography are the best predictors of genus-level misidentification, while phylogeny was the best predictor of species-level misidentifications.

Body size, specifically larger body size, was the best explanation for genus-level misidentification, but not the biological reason for misidentification. *Perognathus parvus* and *Perognathus inornatus*, the two largest *Perognathus* species in this analysis, had the highest misidentification rates of any *Perognathus* species. These species are not only large but also have body size ranges similar to or between other *Chaetodipus* species. The large *Chaetodipus* species also had a high genus-level misidentification rate without size, but this problem was resolved with size. This means that the misidentification was not directly because of allometry, but instead shows evidence of a morphological convergence of large *Perognathus* species to *Chaetodipus* species, which can be explained by their modern biogeographic ranges. *Perognathus parvus* and *Perognathus inornatus* are the only *Perognathus* species in this analysis that do not have a significant overlapping biogeographic range with any *Chaetodipus* species. This suggests that *Perognathus* species body size is influenced by co-occurrence with *Chaetodipus*. In the fossil record, this means we should expect fossil *Perognathus* and *Chaetodipus* body sizes and morphology to vary by geographic co-occurrence.

In the species-level analyses, *Perognathus flavescens* was the only species that had a 100% identification accuracy. This pattern of resolution does not make sense in the context of biogeography. *Perognathus flavescens* is small and has an overlapping biogeographic range with 3 out of the 4 other small *Perognathus* species in the great plains. *Perognathus longimembris* is the geographically separated species, yet these two species were not misidentified for each other. *Perognathus flavescens* is placed as an early-diverging lineage in the Hafner et al., 2007 phylogeny (Fig. 1). In the same phylogeny, *Perognathus flavescens* is also listed as a sister taxon to *Perognathus parvus*, a species that did better with species-level classification than genus-level classification. In this case, the most distantly related species had a higher classification rate at the species-level.

The principal components analyses did not point to one character that can identify *Chaetodipus* and *Perognathus* specimens to genus. Still, there are important characters that represent the morphological diversity of *Chaetodipus* and *Perognathus* specimens. The PCA morphospace and the Generalized Procrustes analysis indicates the premolar and third molar landmarks account for most of the morphological variation. Two important characters appear on the upper premolar: the transverse width of the metaloph and protoloph, and the length of the protoloph enamel-dentin junction. These characters are the geometric morphometric equivalent of the anterior-posterior length and the transverse width of each loph. However, it is not just the size but also the proportions of these measurements that are important for identification. Similarly, an important character for the lower tooth row is the proportional transverse width of the first and second molar relative to the metaloph on the lower premolar. This character

suggests that the occlusal surface length and width ratio of the lower molar is also diagnostic for genus identification.

For the isolated lower premolar, an important character is the median enamel edge of the lophs. In some cases, the lower premolar wore to an “X” shape, where the metaloph and proto-loph converged at a median point. In other cases, the lower premolar lophs diverged, leading to a circular enamel lake. The “X”-shaped wear is a diagnostic feature in this family, but differential wear has never been explored as a diagnostic feature. The morphospace indicates that the wear pattern of the lower premolar could be diagnostic to genus, primarily because the lower tooth row provided a higher classification accuracy than the upper tooth row for identifying specimens to genus. This high classification accuracy in the lower molars provides promise for identifying fossil *Perognathus* and *Chaetodipus* specimens from isolated lower premolars because jaws are more common in the rodent fossil record than palates.

I ran parallel analyses including and excluding size because there is evidence that small mammal body mass changes through time (Bown et al., 1994). The purpose of building this morphospace is to identify fossil *Chaetodipus* and *Perognathus* specimens spanning 20 million years. The analyses with size mostly improved the classification accuracy, but the size ranges of the genera likely change over 20 million years. Because the misidentifications of the genus-level analysis are explained using biogeography, we can expect that excluding scale when analyzing fossil specimens will still provide accurate results, especially in localities with co-occurrences of *Chaetodipus* and *Perognathus* specimens.

This study used modern specimens to test whether a geometric morphometrics landmarking scheme could identify *Chaetodipus* and *Perognathus* to genus using a large dataset while controlling for specimens with complete dentition and young adult wear. Because Miocene and Pliocene species belonging to this clade have conventionally been assigned to *Perognathus* on the assumption that the genera could not be distinguished by dental morphology (Genoways and Brown, 1993), it is quite likely that there are currently older fossil species of *Chaetodipus* incorrectly assigned to *Perognathus*. Conversely, it is also possible that these Miocene and Pliocene specimens are indeed *Perognathus* specimens, which could inform phylogenetic analyses trying to estimate the divergence dates of these two genera. This dataset can now be used to predict the genus identification of unknown fossil specimens using the landmarking scheme presented here. My approach will provide a mechanism for testing the expectation that *Chaetodipus* was also present in mid-Miocene and later fossil assemblages, a result of a 16 million-year-old divergence. This mutual illumination of the fossil and recent records of evolutionary histories is a reminder of how critical modern specimens are for understanding the fossil record.

Figures and Tables

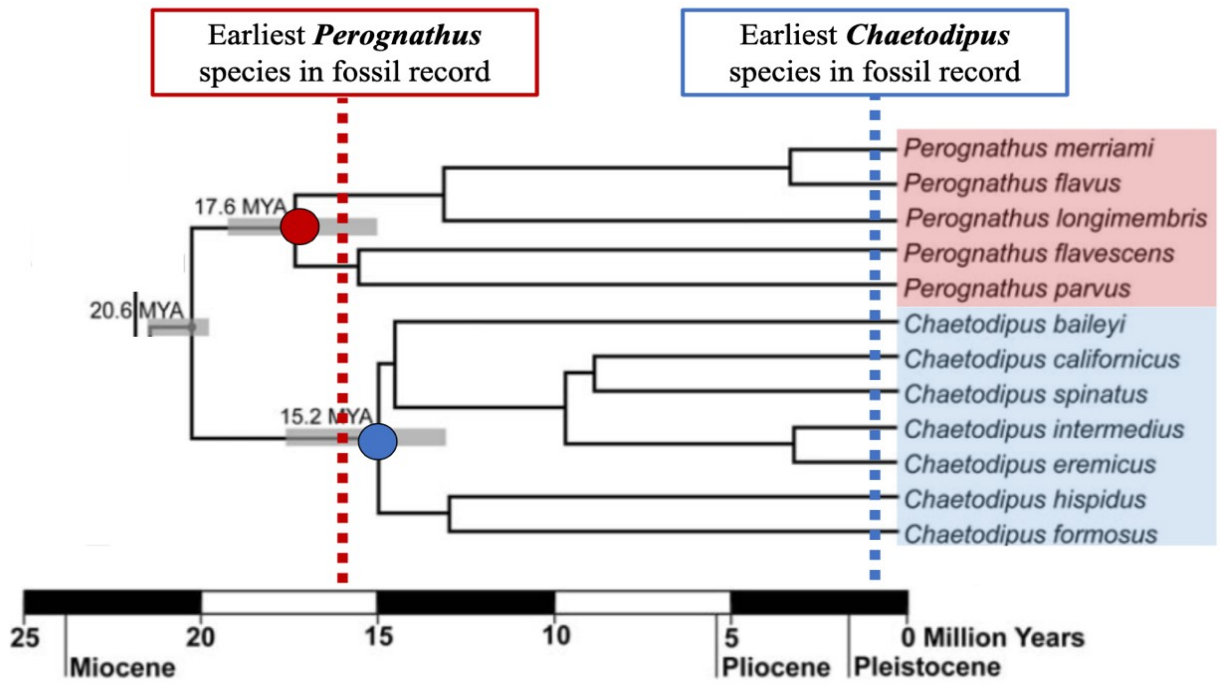


Figure 1. Estimated divergence of *Chaetodipus* and *Perognathus* compared to the fossil record (from Hafner et al., 2007).

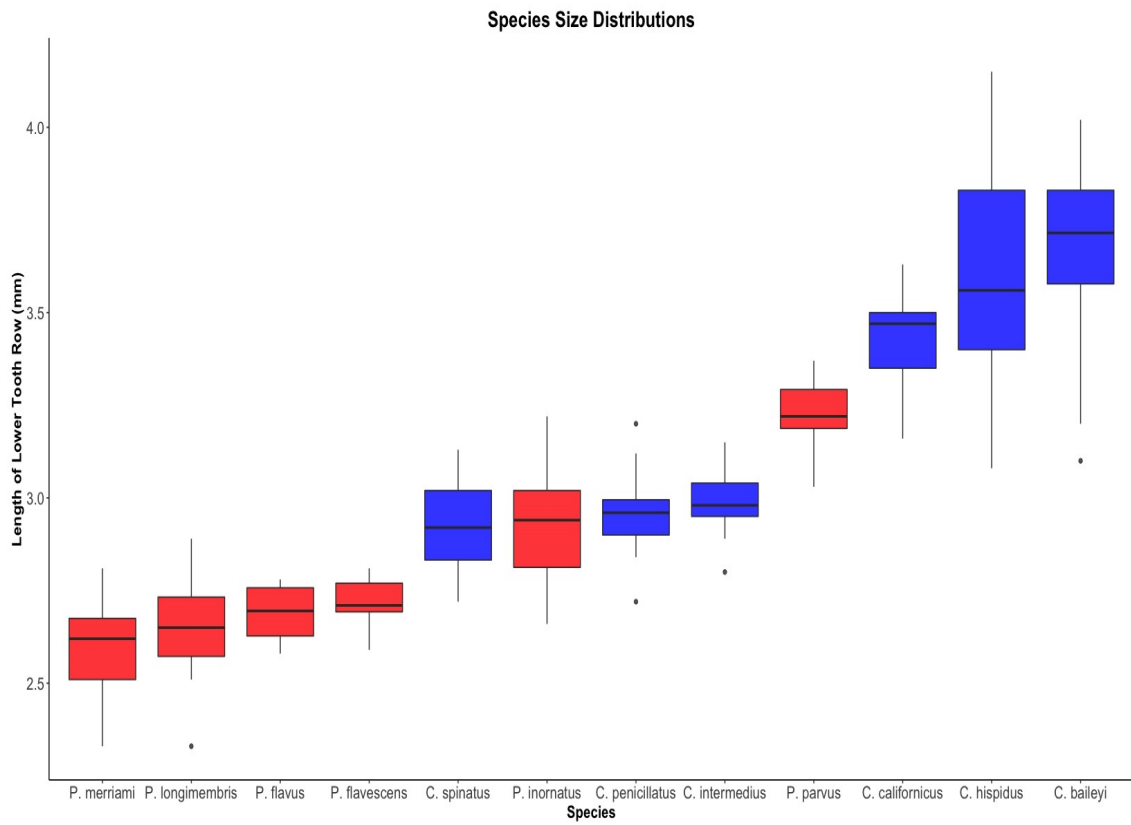


Figure 2: Boxplot of specimen lower tooth row length

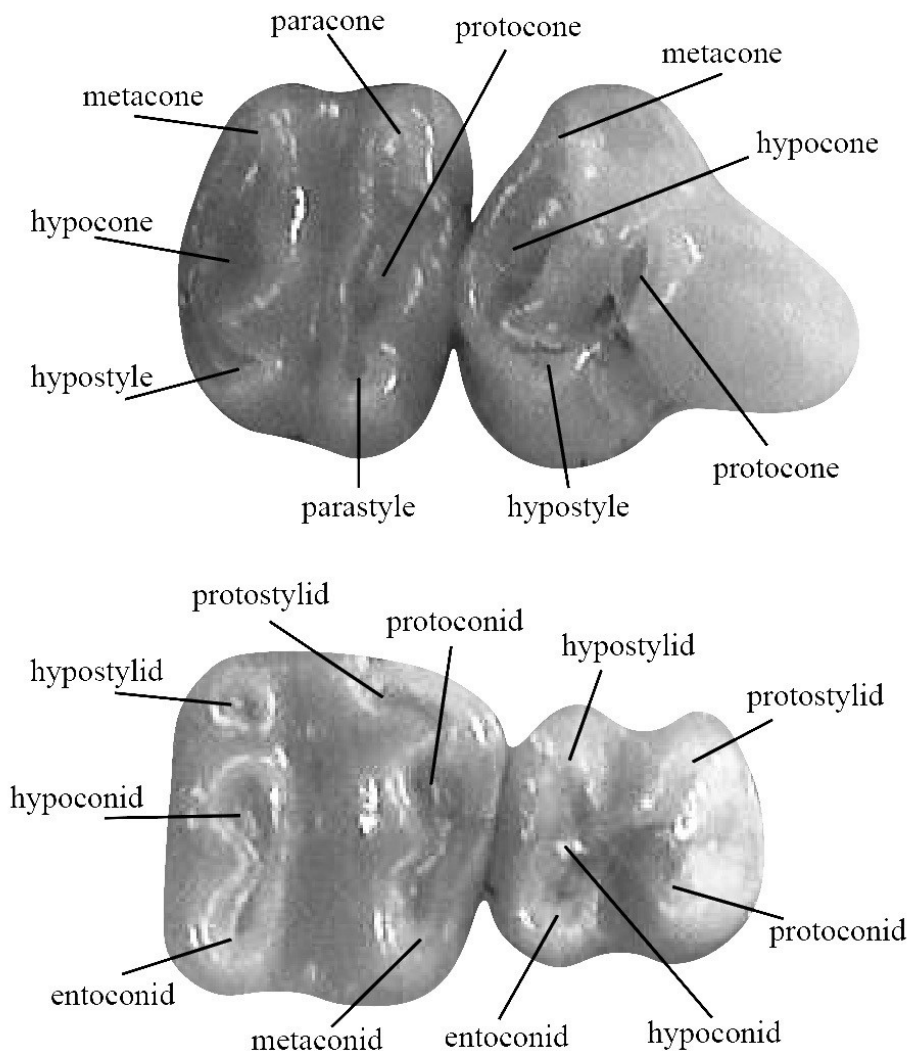


Figure 3. Tooth cusp terminology for molars and premolars

Specimen MVZ 84103 *Chaetodipus hispidus* labeled using cusp terminology in Lindsey, 1973.

Genus	Species	Sample Size
<i>Chaetodipus</i>	<i>baileyi</i>	14
<i>Chaetodipus</i>	<i>californicus</i>	11
<i>Chaetodipus</i>	<i>hispidus</i>	15
<i>Chaetodipus</i>	<i>intermedia</i>	13
<i>Chaetodipus</i>	<i>peninsularis</i>	16

*i
c
i
l
l
a
t
u
s*

<i>Chaetodipus</i>	<i>s</i> <i>p</i> <i>i</i> <i>n</i> <i>a</i> <i>t</i> <i>u</i> <i>s</i>	1 4
<i>Chaetodipus</i>		8 3
<i>Perognathus</i>	<i>f</i> <i>l</i> <i>a</i> <i>v</i> <i>e</i> <i>s</i> <i>c</i> <i>e</i> <i>n</i> <i>s</i>	9
<i>Perognathus</i>	<i>f</i> <i>l</i> <i>a</i> <i>v</i> <i>u</i> <i>s</i>	1 0
<i>Perognathus</i>	<i>i</i> <i>n</i> <i>o</i> <i>r</i> <i>n</i> <i>a</i> <i>t</i> <i>u</i> <i>s</i>	1 4
<i>Perognathus</i>	<i>l</i> <i>o</i> <i>n</i> <i>g</i> <i>i</i> <i>m</i> <i>e</i> <i>m</i> <i>b</i> <i>r</i> <i>i</i> <i>s</i>	1 6
<i>Perognathus</i>	<i>m</i> <i>e</i> <i>r</i> <i>r</i> <i>i</i>	1 5

	a	
	m	
	i	
	p	
<i>Perognathus</i>	r	1
s	v	6
	u	
	s	
<i>Perognathus</i>		8
(total)		0

Table 1: List of specimens used in the analysis

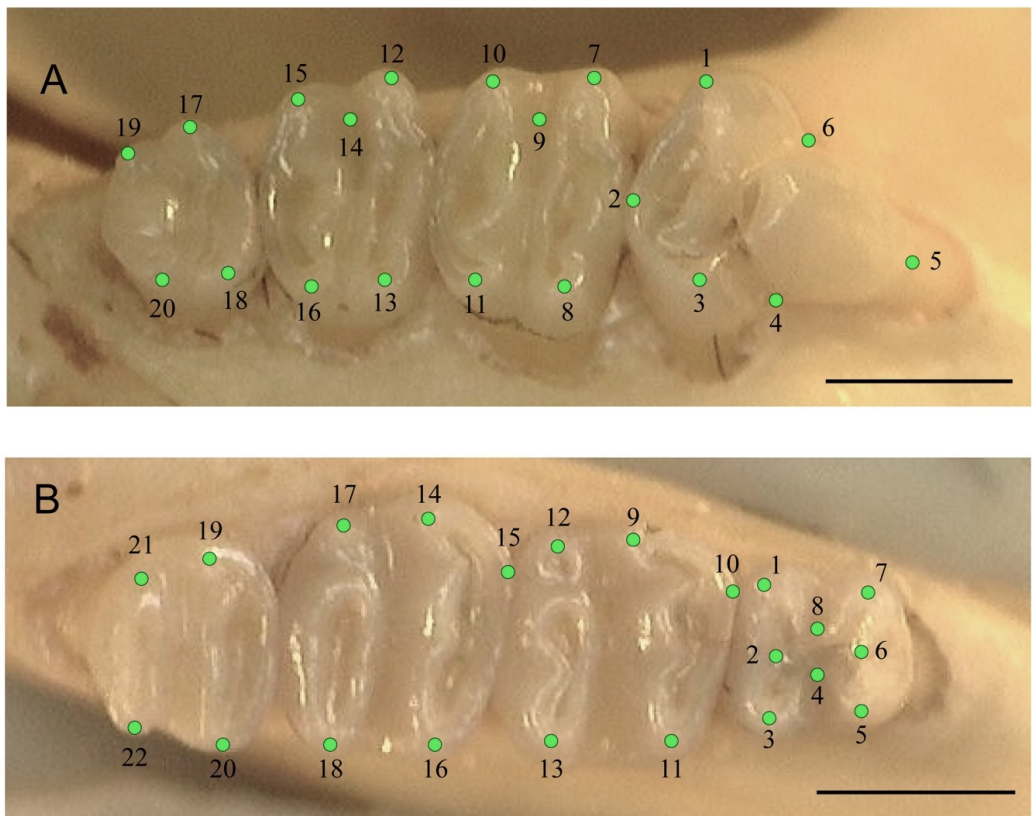


Figure 4: Landmarking scheme for upper molars and lower molars

The landmarks are on MVZ 84103 *Chaetodipus hispidus*. The scale bars are 1 mm.

	Tooth	Landmark	Description
Fig. 2A	P4	1	Buccal edge of the metacone enamel
		2	Posterior edge of the hypocone enamel
		3	Labial edge of the hypostyle enamel
		4	Labial enamel-dentin junction between the metaloph and protoloph
		5	Anterior enamel-dentin junction of the protocone
		6	Buccal enamel-dentin junction between the metaloph and protoloph
	M1	7	Buccal edge of the protoloph enamel
		8	Labial edge of the protoloph enamel
		9	Buccal union of the metaloph and protoloph in the transverse valley
		10	Buccal edge of the metaloph enamel
		11	Labial edge of the metaloph enamel
	M2	12	Buccal edge of the protoloph enamel
		13	Labial edge of the protoloph enamel
		14	Buccal union of the metaloph and protoloph in the transverse valley
		15	Buccal edge of the metaloph enamel
	M3	16	Labial edge of the metaloph enamel
		17	Buccal edge of the protoloph enamel
		18	Labial edge of the protoloph enamel
		19	Buccal edge of the metaloph enamel
		20	Labial edge of the metaloph enamel
Fig. 2B	p4	1	Buccal edge of the metalophid enamel
		2	Posterior enamel edge of the metalophid-protolophid junction
		3	Labial edge of the metalophid enamel
		4	Buccal union of the metalophid and protolophid in the transverse valley
		5	Labial edge of the hypolophid enamel
		6	Anterior enamel edge of the metalophid-protolophid junction
		7	Buccal edge of the hypolophid enamel
		8	Labial union of the metalophid and protolophid in the transverse valley
	m1	9	Buccal edge of the metalophid enamel
		10	Anterior edge of the metalophid
		11	Labial edge of the metalophid enamel
		12	Buccal edge of the hypolophid enamel
		13	Labial edge of the hypolophid enamel
	m2	14	Buccal edge of the metalophid enamel
		15	Anterior edge of the metalophid
		16	Labial edge of the metalophid enamel
		17	Buccal edge of the hypolophid enamel
		18	Labial edge of the hypolophid enamel
	m3	19	Buccal edge of the metalophid enamel
		20	Labial edge of the metalophid enamel
		21	Buccal edge of the hypolophid enamel
		22	Labial edge of the hypolophid enamel

Table 2: Description of landmarks in Figure 4

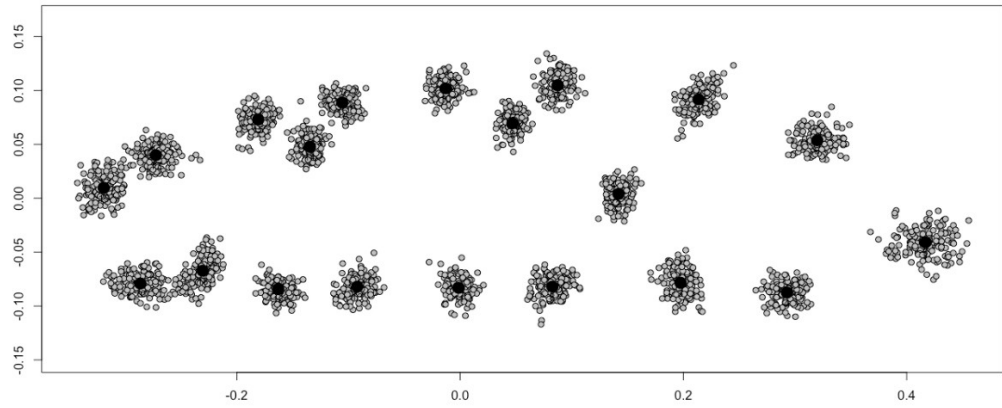


Figure 5: Generalized Procrustes of the upper tooth row

Procrustes normalization of the upper tooth row for both *Chaetodipus* and *Perognathus* specimens. The black dots represent the centroid size and shape used to compare specimens in future analyses.

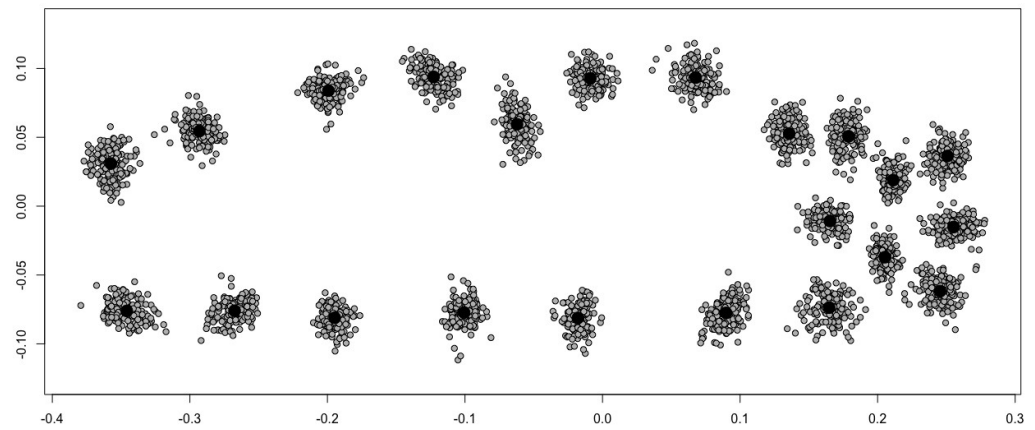


Figure 6: Generalized Procrustes of the lower tooth row

The Procrustes normalization of the lower tooth row for both *Chaetodipus* and *Perognathus* specimens. The black dots represent the centroid size and shape used to compare specimens in future analyses.

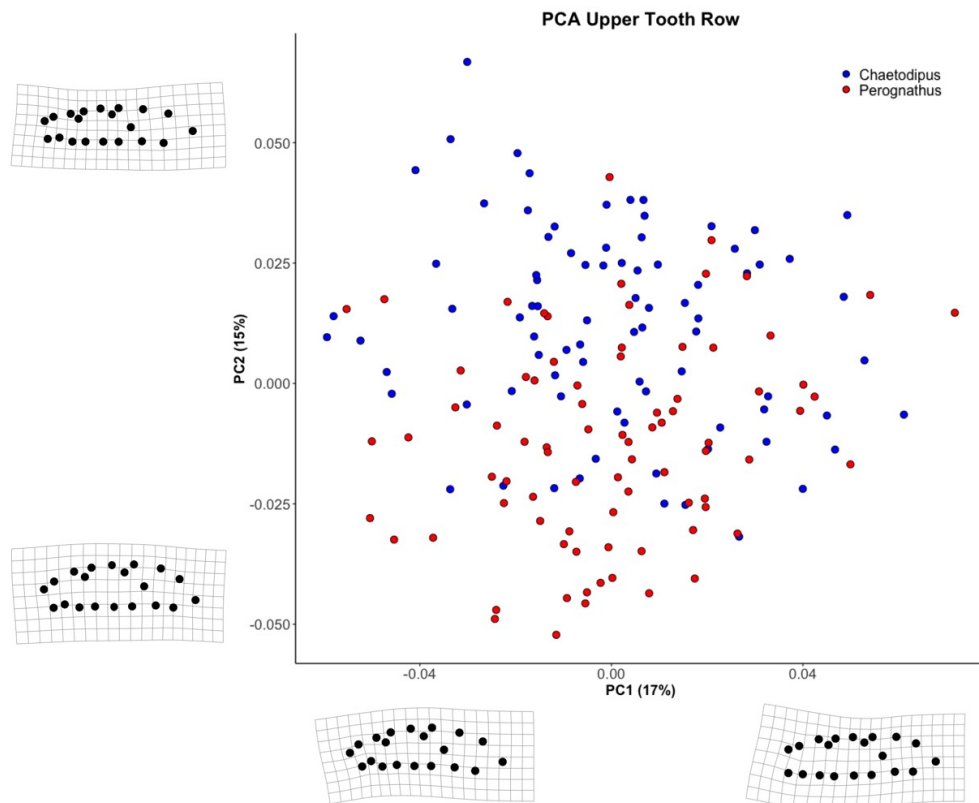


Figure 7: PCA of the upper molars

The principal components analysis of the Procrustes coordinates of the upper molars of the *Chaetodipus* (blue) and *Perognathus* (red) specimens. Principal Component 1 (x-axis) accounts for 17% of the variation among specimens, Principal Component 2 (y-axis) accounts for 15% of the variation between specimens. The principal component minimum and maximum are shown next to the axes.

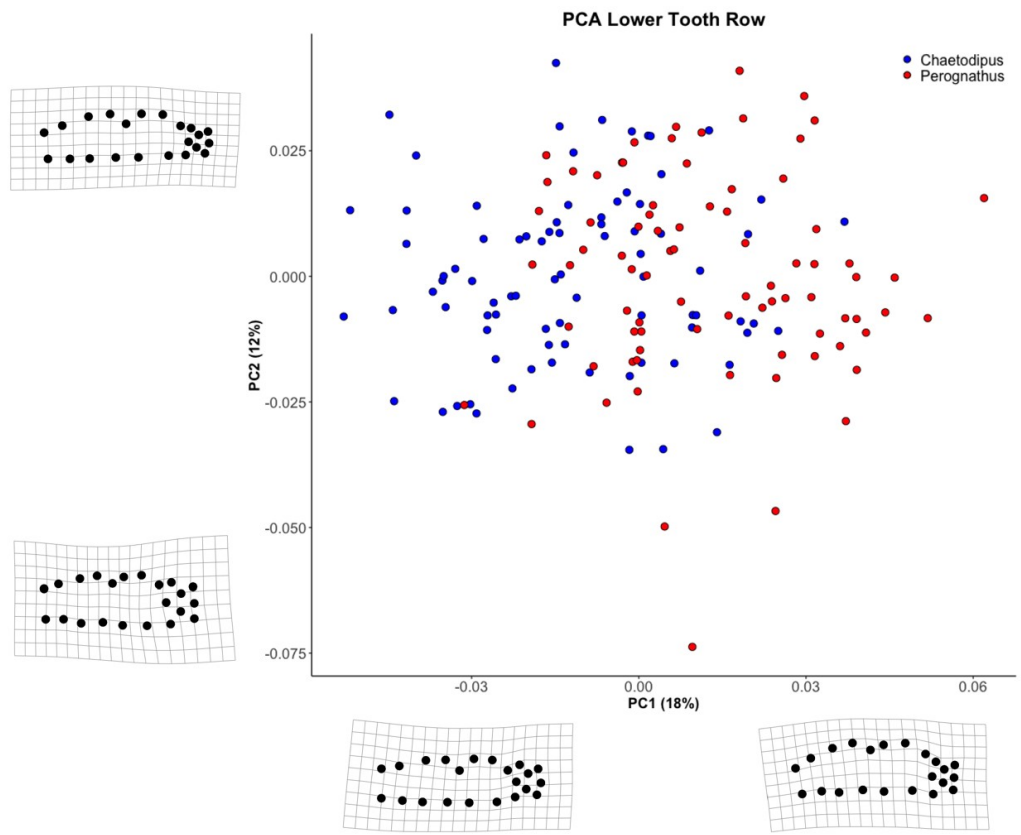


Figure 8: PCA of lower molars

The principal components analysis of the Procrustes coordinates of the lower molars of the *Chaetodipus* (blue) and *Perognathus* (red) specimens. Principal Component 1 (x-axis) accounts for 18% of the variation among specimens, Principal Component 2 (y-axis) accounts for 12% of the variation between specimens. The principal component minimum and maximum are shown next to the axes.

Classification Level (n=number of groups)	Teeth in Dataset	Classification accuracy without size	Classification accuracy with size
Genus (n=2)	upper and lower molars	91%	92%
Genus (n=2)	upper tooth row	82%	87%
Genus (n=2)	upper P4	79%	84%
Genus (n=2)	lower tooth row	86%	87%
Genus (n=2)	lower p4	69%	79%
Species (n=12)	upper and lower molars	61%	72%
Species (n=12)	upper tooth row	47%	63%
Species (n=12)	upper P4	27%	56%
Species (n=12)	lower tooth row	49%	60%
Species (n=12)	lower p4	26%	38%

Table 3: Summary table of canonical variates analyses

The table shows a summary of multiple canonical variates analyses using different sets of tooth landmarks and assigning different groups. Groups are either the number of genera or the number of species being distinguished in an analysis. The analyses use all of the landmarks in the tooth row or only the premolar.

Complete Dentition

With Size		Without Size	
Species	Freq Wrong	Species	Freq Wrong
<i>P. parvus</i>	3	<i>P. parvus</i>	4
<i>P. longimembris</i>	2	<i>C. baileyi</i>	3
<i>C. hispidus</i>	1	<i>C. hispidus</i>	3
<i>C. penicillatus</i>	1	<i>P. longimembris</i>	2
<i>P. flavescens</i>	1	<i>C. penicillatus</i>	1
<i>P. flavus</i>	1	<i>C. spinatus</i>	1
<i>P. inornatus</i>	1	<i>P. flavescens</i>	1
		<i>P. flavus</i>	1
		<i>P. inornatus</i>	1

Upper Tooth Row

With Size		Without Size	
Species	Freq wrong	Species	Freq Wrong
<i>P. inornatus</i>	7	<i>P. inornatus</i>	6
<i>P. parvus</i>	6	<i>P. parvus</i>	6
<i>C. intermedius</i>	2	<i>C. baileyi</i>	4
<i>P. longimembris</i>	1	<i>C. hispidus</i>	4
<i>P. flavus</i>	1	<i>C. californicus</i>	2
<i>C. baileyi</i>	1	<i>C. penicillatus</i>	1
<i>C. hispidus</i>	1	<i>P. flavescens</i>	1
<i>P. flavescens</i>	1	<i>P. flavus</i>	1
		<i>P. merriami</i>	1

Lower Tooth Row

With Size		Without Size	
Species	Freq Wrong	Species	Freq Wrong
<i>P. inornatus</i>	7	<i>P. inornatus</i>	7
<i>C. penicillatus</i>	5	<i>C. penicillatus</i>	5
<i>P. parvus</i>	3	<i>P. parvus</i>	3
<i>C. intermedius</i>	2	<i>P. longimembris</i>	2
<i>P. longimembris</i>	2	<i>C. baileyi</i>	1
<i>C. baileyi</i>	1	<i>C. hispidus</i>	1
<i>P. flavus</i>	1	<i>C. intermedius</i>	1
		<i>P. flavus</i>	1

Table 4. Summary of misidentification from genus-level cross-validation

predicted \ actual	<i>C. baileyi</i>	<i>C. californicus</i>	<i>C. hispidus</i>	<i>C. intermedius</i>	<i>C. penicillatus</i>	<i>C. spinatus</i>	<i>P. flavus</i>	<i>P. inornatus</i>	<i>P. longimembra</i>	<i>P. merriami</i>	<i>P. parvus</i>	Sample size
<i>C. baileyi</i>	6	3	1	1	0	2	0	1	0	0	0	14
<i>C. californicus</i>	2	4	0	0	1	2	0	2	0	0	0	11
<i>C. hispidus</i>	0	1	12	0	1	1	0	0	0	0	0	15
<i>C. intermedius</i>	0	0	0	11	1	1	0	0	0	0	0	13
<i>C. penicillatus</i>	1	1	2	0	6	3	0	3	0	0	0	16
<i>C. spinatus</i>	3	0	1	1	0	9	0	0	0	0	0	14
<i>P. flavus</i>	0	0	0	0	0	0	9	0	0	0	0	9
<i>P. inornatus</i>	0	0	0	0	0	0	0	5	0	0	0	10
<i>P. longimembra</i>	1	0	0	0	1	2	0	4	2	1	3	14
<i>P. merriami</i>	0	0	0	0	0	0	0	3	12	1	0	16
<i>P. parvus</i>	0	0	0	0	0	0	1	1	1	10	2	15
<i>P. parvus</i>	0	1	0	0	0	1	0	2	0	0	12	16

Table 5:
Summary table of species-level classification accuracy from complete dentition without size

Each number is the frequency of identifications with the horizontal rows adding up to the sample size of each species. Row titles are the known specimen identification, and the column titles are the predicted identifications. The correctly identified frequencies are in green.

predicted \ actual	<i>C. baileyi</i>	<i>C. californicus</i>	<i>C. hispidus</i>	<i>C. intermedius</i>	<i>C. penicillatus</i>	<i>C. spinatus</i>	<i>P. flavescens</i>	<i>P. flavus</i>	<i>P. inornatus</i>	<i>P. longimembris</i>	<i>P. merriami</i>	<i>P. parvus</i>	Sample size
<i>C. baileyi</i>	10	2	1	0	0	1	0	0	0	0	0	0	14
<i>C. californicus</i>	2	6	2	0	0	1	0	0	0	0	0	0	11
<i>C. hispidus</i>	1	3	10	0	1	0	0	0	0	0	0	0	15
<i>C. intermedius</i>	0	0	0	9	1	1	0	0	1	0	1	0	13
<i>C. penicillatus</i>	0	1	0	1	10	2	0	0	2	0	0	0	16
<i>C. spinatus</i>	0	0	0	1	0	13	0	0	0	0	0	0	14
<i>P. flavescens</i>	0	0	0	0	0	0	9	0	0	0	0	0	9
<i>P. flavus</i>	0	0	0	0	0	0	0	4	0	0	0	0	10
<i>P. inornatus</i>	0	0	0	1	1	1	0	0	8	1	2	0	14
<i>P. longimembris</i>	0	0	0	1	0	0	0	0	2	12	1	0	16
<i>P. merriami</i>	0	0	0	0	0	0	0	2	0	1	12	0	15
<i>P. parvus</i>	0	0	0	0	0	1	0	0	1	0	0	14	16

Table 6: Summary table of species-level classification accuracy from complete dentition with size

Each number is the frequency of identifications with the horizontal rows adding up to the sample size of each species. Row titles are the known specimen identification, and the columns titles are the predicted identifications. The correctly identified frequencies are in green.

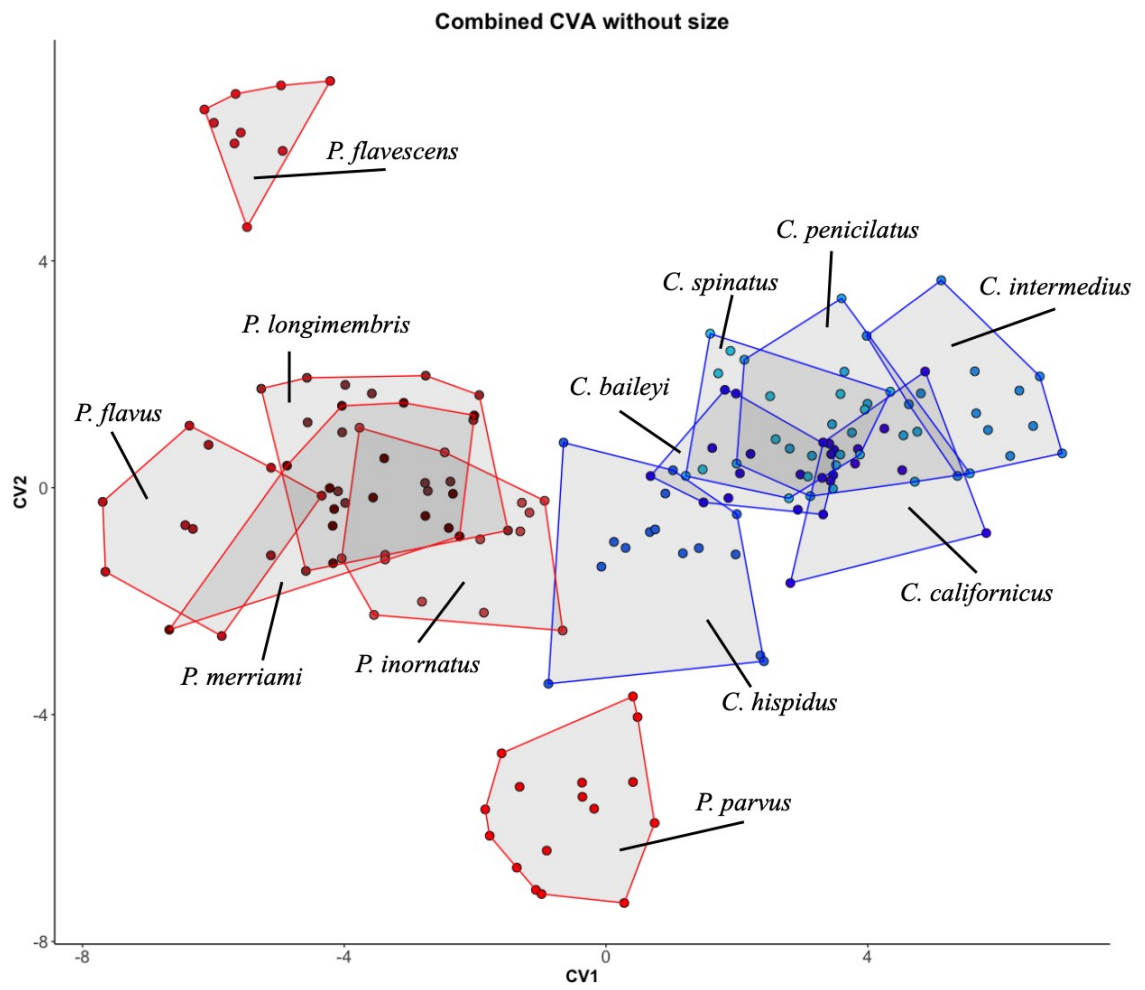


Figure 9: Canonical variates analysis of species complete dentition without size

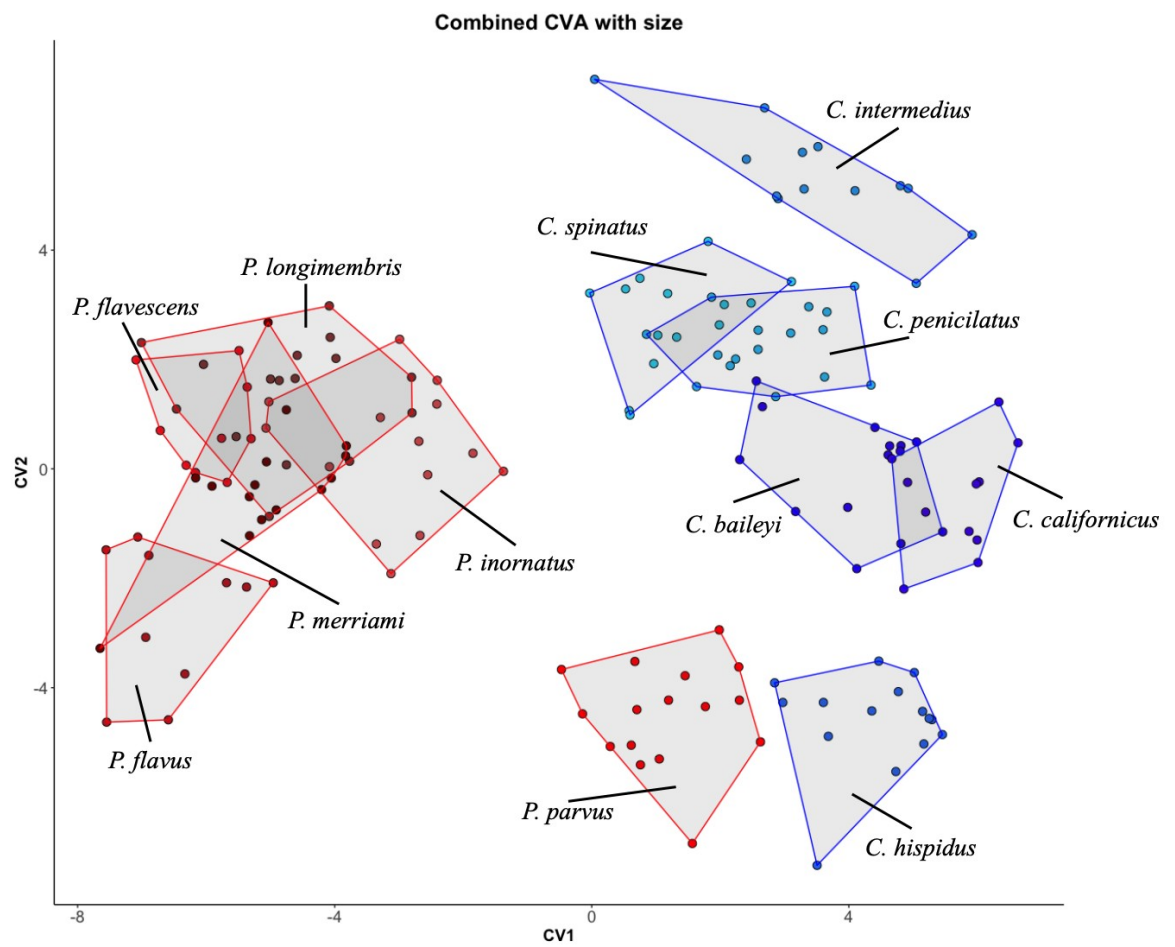


Figure 10: Canonical variates analysis of species complete dentition with size

Bibliography

- ADAMS, D. C., M. L. COLLYER, AND A. KALIONTZOPOULOU. 2018. Geomorph: Software for geometric morphometric analyses. R package version 3.0.7. <https://cran.r-project.org/package=geomorph>
- AYER, M. 1936. The Archaeological and Faunal Material from Williams Cave, Guadalupe Mountains, Texas. *Proceedings of the Academy of Natural Sciences of Philadelphia* 18:599–618.
- BARNOSKY, A. D. 1986. New species of the Miocene rodent *Cupidinimus* (Heteromyidae) and some evolutionary relationships within the genus. *Journal of Vertebrate Paleontology* 6:46–64.
- BOWN, T. M., P. A. HOLROYD, AND K. D. ROSE. 1994. Mammal extinctions, body size, and paleotemperature. *Proceedings of the National Academy of Sciences* 91:10403–10406.
- CALEDE, J. J. M., AND J. W. GLUSMAN. 2017. Geometric morphometric analyses of worn cheek teeth help identify extant and extinct gophers (Rodentia, Geomyidae). *Palaeontology* 60:281–307.
- CARRASCO, M. A. 2000. Species discrimination and morphological relationships of kangaroo rats (*Dipodomys*) based on their dentition. *Journal of Mammalogy* 81:16.
- FRUCIANO, C. 2016. Measurement error in geometric morphometrics. *Development Genes and Evolution* 226:139–158.
- GENOWAYS, H., AND J. BROWN (EDS.). 1993. *Biology of the Heteromyidae*. American Society of Mammalogists.
- GINGERICH, P. D. 1974. Size Variability of the Teeth in Living Mammals and the Diagnosis of Closely Related Sympatric Fossil Species. *Journal of Paleontology* 48:895–903.
- HOFFMEISTER, D. F., AND M. R. LEE. 1967. Revision of the Pocket Mice, *Perognathus penicillatus*. *Journal of Mammalogy* 48:361.
- KLINGENBERG, C. P. 2016. Size, shape, and form: concepts of allometry in geometric morphometrics. *Development Genes and Evolution* 226:113–137.
- KORTH, W. W. 1987. New rodents (Mammalia) from the late Barstovian (Miocene) Valentine Formation, Nebraska. *Journal of Paleontology* 61:1058–1064.

- KORTH, W. W. 2008. Two new pocket mice (Mammalia, Rodentia, Heteromyidae) from the Miocene of Nebraska and New Mexico and the early evolution of the subfamily Perognathinae. *Geodiversitas* 30:593–609.
- LINDSAY, E. 1972. *Small Mammal Fossils from the Barstow Formation, California*. University of California Press.
- LOSOS, J. B. 2011. Seeing the Forest for the Trees: The Limitations of Phylogenies in Comparative Biology: (American Society of Naturalists Address). *The American Naturalist* 177:709–727.
- MCGUIRE, J. L. 2011. Identifying California *Microtus* species using geometric morphometrics documents Quaternary geographic range contractions. *Journal of Mammalogy* 92:1383–1394.
- MERRIAM, C. H. 1889. Preliminary Revision of the North American Pocket Mice. *North American Fauna* 1:1–36.
- R CORE TEAM. 2018. *R: A Language and Environment for Statistical Computing*. R Foundation for Statistical Computing, Vienna, Austria. <http://www.R-project.org>
- RABOSKY, D. L. 2010. Extinction rates should not be estimated from molecular phylogenies. *Evolution* 64:1816–1824.
- REYNOLDS, R. E. 1992. Miocene vertebrates in the Little Piute Mountains, Southeastern Mojave Desert. *San Bernardino County Museum Special Publication* 92:92–94.
- ROHLF, F. J. 2018. tpsDig2.31. Department of Ecology and Evolution at Stony Brook University. <http://life.bio.sunysb.edu/morph/index.html>
- ROHLF, F. J. 2019. tpsUtil1.79. Department of Ecology and Evolution at Stony Brook University. <http://life.bio.sunysb.edu/morph/index.html>
- SCHLAGER, S. 2017. Morpho and Rvcg: Shape Analysis in R. R package version 2.8. <https://cran.r-project.org/package=Morpho>
- SLATER, G. J., L. J. HARMON, AND M. E. ALFARO. 2012. Integrating fossils with molecular phylogenies improves inference of trait evolution. *Evolution* 66:3931–3944.
- SMITH, S. M., AND G. P. WILSON. 2017. Species Discrimination of Co-Occurring Small Fossil Mammals: A Case Study of the Cretaceous-Paleogene Multituberculate Genus *Mesodma*. *Journal of Mammalian Evolution* 24:147–157.
- WEBSTER, M. 2010. A practical introduction to landmark-based geometric morphometrics. *The Paleontological Society Papers* 16:163–188.

WOOD, A. 1935. Evolution and Relationship of Heteromyid Rodents. *Annals of the Carnegie Museum* 24:73-262

WOOD, A. E. 1933. A New Heteromyid Rodent from the Oligocene of Montana. *Journal of Mammalogy* 14:134.

ZELDITCH, M. (ED.). 2004. *Geometric morphometrics for biologists: a primer*. Elsevier Academic Press.